

Response of GN Type II and Type III Theories on Reflection and Transmission Coefficients at the Boundary Surface of Micropolar Thermoelastic Media with Two Temperatures

R. Kumar¹, M. Kaur^{2,*}, S.C. Rajvanshi³

¹Department of Mathematics, Kurukshetra University, Kurukshetra 136119, India

²Department of Applied Sciences, Guru Nanak Dev Engineering College, Ludhiana, Punjab 141008, India

³Department of Applied Sciences, Gurukul Vidyapeeth Institute of Engineering and Technology, Sector-7, Banur, District Patiala, Punjab 140601, India

Received 1 August 2014; accepted 9 October 2014

ABSTRACT

In the present article, the reflection and transmission of plane waves at the boundary of thermally conducting micropolar elastic media with two temperatures is studied. The theory of thermoelasticity with and without energy dissipation is used to investigate the problem. The expressions for amplitudes ratios of reflected and transmitted waves at different angles of incident wave are obtained. Dissipation of energy and two temperature effects on these amplitude ratios with angle of incidence are depicted graphically. Some special and particular cases are also deduced.

© 2014 IAU, Arak Branch. All rights reserved.

Keywords: Micropolar thermoelastic media; Two temperatures; Reflection and transmission coefficients; Amplitude ratios; Energy dissipation.

1 INTRODUCTION

THE theory of micropolar elasticity was introduced and developed by Eringen [1]. The theory of micropolar continuum mechanics gives consideration to the microstructure. Micropolar theory is useful in structure materials with a fibrous, lattice or granular micropolar structure. The main difference of micropolar elastic material from the classical elastic material is that each point has extra rotational degrees of freedom independent of translation and the material can transmit couple as well as usual force stress.

The linear theory of micropolar thermoelasticity has been developed by extending the theory of micropolar continua. A comprehensive review of works on the subject was due to Eringen [2] and Nowacki [3]. Dost and Taborok [4] presented the generalized thermoelasticity by using Green and Lindsay theory. Chandrasekharaiah [5] developed a heat flux dependent micropolar thermoelasticity. Boschi and Iesan [6] extended a generalized theory of micropolar thermoelasticity that permits the transmission of heat as thermal waves at finite speed.

Thermoelasticity with two temperatures is one of the non-classical theories of thermodynamics of elastic solids. The main difference of this theory with respect to classical one is in the thermal dependence. Boley and Tolins [7] while studying the transient coupled thermoelastic boundary-value problem in half-space concluded that two temperatures and strains are the foundation of the results in the form of the wave-pulse response which occurs instantaneously throughout the body. In the theory of thermodynamics, the temperature caused by the thermal process is known as

* Corresponding author. Tel.: +91 9463055900.

E-mail address: mandeep1125@yahoo.com (M. Kaur).

conductive temperature Φ and the temperature due to mechanical process in the material is known as thermodynamic temperature T . Chen et al. [8-9] have formulated a theory of heat conduction in deformable bodies, which depend on two distinct temperatures, the conductive temperature Φ and thermodynamic temperature T . For time-independent situations, the difference between these two temperatures is proportional to the heat supply while the two temperatures are identical in the absence of any heat supply. For time-dependent problems, however, and for wave propagation problems in particular, the two temperatures are in general different regardless of the presence of a heat supply. The two temperatures and the strain are found to have representation in the form of a travelling wave pulse, a response which occurs instantaneously throughout the body (Boley [10]). The wave propagation in the two temperature theory of thermoelasticity was investigated by Warren and Chen [11].

A new theory of generalized thermoelasticity by taking into account the theory of heat conduction in deformable bodies, which depends on distinct conductive and thermodynamic temperatures and a uniqueness theorem for the equation of two temperatures generalized linear thermoelasticity for a homogeneous and isotropic body was presented by Youssef [12]. Various investigators Kumar and Mukhopadhyay [13], Kaushal et al. [14], Ezzat and Awad [15], Kaushal et al. [16], El-Karamany and Ezzat [17], Banik and Kanoria [18] studied different problems in thermoelastic media with two temperatures. Kumar and Abbas [19] studied deformation due to thermal source in micropolar thermoelastic media with thermal and conductive temperatures, Youssef [20] studied state-space approach to two-temperature generalized thermoelasticity without energy dissipation of medium subjected to moving heat source. Ailawalia and Lofty [21] studied two temperature generalized magneto-thermoelastic interactions in an elastic medium under three theories.

To study the propagation of thermal waves at finite speed, it may be possible in the foreseeable future to identify an idealized material. Green and Naghdi [22-24] has made relevant theoretical development in the theory of thermoelasticity and provided sufficient basic modifications in the constitutive equations that allow treatment of wider class of heat flow problems, labeled as types I, II, III. When the respective theories are linearized, type I is similar to classical heat equation, whereas the linearized version of type II and type III theories allow propagation of thermal waves at finite speed. In type II and type III (i.e. thermoelasticity without energy dissipation and thermoelasticity with energy dissipation) the entropy flux vector is determined in terms of potential that also determine stresses. The temperature equation reduces to classical Fourier law of heat conduction when Fourier conductivity is dominant; and when the effect of conductivity is negligible, the equation has undamped thermal wave solutions without energy dissipation.

Various investigators have studied the different problems using GN type II and type III theories notable among them are Taheri et al. [25], Mukhopadhyay and Kumar [26], Mohamed et al. [27], Chrita and Ciarletta [28-29], Passarella and Zampoli [30]. Abbas [31] investigated GN model for thermoelastic interaction in an unbounded fiber-reinforced anisotropic medium with a circular hole. Ailawalia et al. [32] studied dynamic problem in Green-Naghdi (Type III) thermoelastic half-space with two temperature. Das et al. [33] studied a problem of magneto-thermoelastic interactions in a transversely isotropic hollow cylinder due to thermal shock in the context of three phase-lag theory of generalized thermoelasticity. Kothari and Mukhopadhyay [34] presented some theorems in the linear theory of thermoelasticity with dual phase-lags for an anisotropic and in homogeneous material. Othman et al. [35] discussed the effect of gravity on plane waves in generalized thermo-microstretch elastic solid under Green Naghdi theory. Fahmy [36] studied the generalized magneto-thermo-viscoelastic problem in a rotating solid of functionally graded material (FGM) in the context of the Green and Naghdi theory of type III. El-Karamany and Ezzat [37] proved the uniqueness and reciprocal theorems are without the use of Laplace transforms for the Dual-Phase-Lag thermoelasticity theory. Guo et al. [38] investigates the thermoelastic dissipation of micro-plate resonators by using the generalized thermoelasticity theory of dual-phase-lagging model.

In the present investigation, we study the reflection and transmission of plane waves i.e. longitudinal displacement wave (LD wave), thermal wave (T wave), transverse displacement wave coupled with microrotational wave (CD-I wave and CD-II wave) at the boundary of thermally conducting micropolar elastic media with two temperatures with and without energy dissipation. Energy dissipation and two temperature effects are depicted numerically and depicted graphically on the amplitude ratios for incidence of various plane waves for a particular model.

2 BASIC EQUATIONS

The field equations in an isotropic, homogeneous, micropolar elastic medium following Eringen [1], Ezzat and The field equations in an isotropic, homogeneous, micropolar elastic medium following Eringen [1], Ezzat and Awad

[15] and Green and Naghdi [23] in the theory of thermoelasticity with energy dissipation, without body forces, body couples and heat sources, are given by

$$(\lambda + \mu)u_{j,ij} + (\mu + K)u_{i,ij} + K\varepsilon_{ijk}\phi_{k,j} - \nu(\Phi - a\Phi_{,ij})_{,i} = \rho\ddot{u}_i, \quad (1)$$

$$(\alpha + \beta)\phi_{j,ij} + \gamma\phi_{i,ij} + K\varepsilon_{imn}u_{n,m} - 2K\phi_i = \rho j\ddot{\phi}_i, \quad (2)$$

$$K_1\Phi_{,rr} + K_1^*\nabla^2\Phi_{,rr} = \rho c^*(\ddot{\Phi} - a\ddot{\Phi}_{,ij}) + \nu T_0\ddot{u}_{j,j}, \quad (3)$$

and the constitutive relations are

$$t_{ij} = \lambda u_{r,r}\delta_{ij} + \mu(u_{i,j} + u_{j,i}) + K(u_{j,i} - \varepsilon_{ijr}\phi_r) - \nu T\delta_{ij}, \quad (4)$$

$$m_{ij} = \alpha\phi_{r,r}\delta_{ij} + \beta\phi_{i,j} + \gamma\phi_{j,i}, \quad i, j, r = 1, 2, 3 \quad (5)$$

where λ and μ are Lamé's constants. K, α, β and γ are micropolar constants. t_{ij} and m_{ij} are the components of stress tensor and couple stress tensor. u_i and ϕ_i are the displacement and microrotation vectors, ρ is the density, j is the microinertia, K_1^* is the thermal conductivity, $K_1 = \frac{c^*(\lambda + 2\mu)}{4}$ is material characteristics constant of the theory, c^* is the specific heat at constant strain, Φ is the deviation of conductive temperature from reference temperature, T is the deviation of thermodynamic temperature from reference temperature, T_0 is the reference temperature, $\nu = (3\lambda + 2\mu + K)\alpha_T$, where α_T is the coefficient of linear thermal expansion, δ_{ij} is the Kronecker delta, ε_{ijr} is the alternating tensor. T and Φ are connected by the relation $T = (1 - a\nabla^2)\Phi$, where a is a two temperature parameter.

3 FORMULATION OF THE PROBLEM

Two homogeneous, isotropic, micropolar, thermoelastic solid half spaces with two temperatures (medium M_1) and (medium M_2) in contact with each other are considered. Origin of the rectangular Cartesian co-ordinate system $Ox_1x_2x_3$ is taken on the surface $x_3 = 0$ and x_3 -axis is pointing normally into the medium M_1 .

The components of displacement and microrotation for two dimensional problem are taken in the form

$$u = (u_1(x_1, x_3), 0, u_3(x_1, x_3)), \quad \varphi = (0, \phi_2(x_1, x_3), 0) \quad (6)$$

Eqs. (1)-(3) with the help of Eq. (6), reduce to the following equations

$$(\lambda + \mu)\frac{\partial e_1}{\partial x_1} + (\mu + K)\nabla^2 u_1 - K\frac{\partial \phi_2}{\partial x_3} - \nu(1 - a\nabla^2)\frac{\partial \Phi}{\partial x_1} = \rho\frac{\partial^2 u_1}{\partial t^2}, \quad (7)$$

$$(\lambda + \mu)\frac{\partial e_1}{\partial x_3} + (\mu + K)\nabla^2 u_3 + K\frac{\partial \phi_2}{\partial x_1} - \nu(1 - a\nabla^2)\frac{\partial \Phi}{\partial x_3} = \rho\frac{\partial^2 u_3}{\partial t^2}, \quad (8)$$

$$\gamma\nabla^2\phi_2 + K\left(\frac{\partial u_1}{\partial x_3} - \frac{\partial u_3}{\partial x_1}\right) - 2K\phi_2 = \rho j\frac{\partial^2 \phi_2}{\partial t^2}, \quad (9)$$

$$(K_1 + K_1^*\frac{\partial}{\partial t})\nabla^2\Phi = \rho c^*\frac{\partial^2}{\partial t^2}(1 - a\nabla^2)\Phi + \nu T_0\frac{\partial^2}{\partial t^2}e_1, \quad (10)$$

where

$$e_1 = \left(\frac{\partial u_1}{\partial x_1} + \frac{\partial u_3}{\partial x_3} \right), \nabla^2 = \frac{\partial^2}{\partial x_1^2} + \frac{\partial^2}{\partial x_3^2}.$$

The dimensionless quantities are defined as:

$$\begin{aligned} x_1' &= \frac{x_1}{L}, & x_3' &= \frac{x_3}{L}, & u_1' &= \frac{u_1}{L}, & u_3' &= \frac{u_3}{L}, & \phi_2' &= \frac{\lambda}{\nu T_0} \phi_2, & t' &= \frac{c_1}{L} t, \\ T' &= \frac{T}{T_0}, & \Phi' &= \frac{\Phi}{T_0}, & t_{ij}' &= \frac{1}{\nu T_0} t_{ij}, & m_{ij}' &= \frac{1}{L \nu T_0} m_{ij}, & a' &= \frac{1}{L} a \end{aligned} \quad (11)$$

where $\omega^* = \frac{\rho c^* c_1^2}{K^*}$, $c_1^2 = \frac{\lambda + 2\mu + K}{\rho}$, L is a parameter having dimensions of length.

The relations between non-dimensional displacement components u_1, u_3 and the dimensionless potential functions ϕ, ψ can be expressed as:

$$u_1 = \frac{\partial \phi}{\partial x_1} - \frac{\partial \psi}{\partial x_3}, \quad u_3 = \frac{\partial \phi}{\partial x_3} + \frac{\partial \psi}{\partial x_1}, \quad (12)$$

Making use of Eq. (11) in Eqs. (7)-(10) and with the aid of Eq. (12) after suppressing the primes, we obtain

$$a_3 \nabla^2 \phi - a_2 (1 - a \nabla^2) \Phi - a_3 \frac{\partial^2 \phi}{\partial t^2} = 0, \quad (13)$$

$$\nabla^2 \psi + a_1 \phi_2 - a_3 \frac{\partial^2 \psi}{\partial t^2} = 0, \quad (14)$$

$$\nabla^2 \phi_2 - a_4 \nabla^2 \psi - 2a_5 \phi_2 - a_6 \frac{\partial^2 \phi_2}{\partial t^2} = 0, \quad (15)$$

$$[\nabla^2 (1 + a_7 \frac{\partial}{\partial t}) - a_8 \frac{\partial^2}{\partial t^2} (1 - a \nabla^2)] \Phi - a_9 \frac{\partial^2}{\partial t^2} \nabla^2 \phi = 0, \quad (16)$$

where

$$\begin{aligned} a_1 &= \frac{K \nu T_0}{(\mu + K) \lambda}, & a_2 &= \frac{\nu T_0}{\mu + K}, & a_3 &= \frac{\rho c_1^2}{\mu + K}, & a_4 &= \frac{K L^2 \lambda}{\gamma \nu T_0}, & a_5 &= \frac{K L^2}{\gamma}, & a_6 &= \frac{\rho j c_1^2}{\gamma}, & a_7 &= \frac{K_1^* c_1}{K_1 L}, \\ a_8 &= \frac{\rho c^* c_1^2}{K_1}, & a_9 &= \frac{\nu c_1^2}{K_1}. \end{aligned}$$

4 BOUNDARY CONDITION

The following boundary conditions at the interface $x_3=0$ are considered

$$t_{33} = \bar{t}_{33}, \quad t_{31} = \bar{t}_{31}, \quad m_{32} = \bar{m}_{32}, \quad u_1 = \bar{u}_1, \quad u_3 = \bar{u}_3, \quad \phi_2 = \bar{\phi}_2, \quad \Phi = \bar{\Phi}, \quad (K_1 + K_1^* \frac{\partial}{\partial t}) \frac{\partial \Phi}{\partial x_3} = (\bar{K}_1 + \bar{K}_1^* \frac{\partial}{\partial t}) \frac{\partial \bar{\Phi}}{\partial x_3} \quad (17)$$

5 REFLECTION AND TRANSMISSION

We consider longitudinal displacement wave (LD-wave), thermal wave (T-wave), transverse displacement wave coupled with microrotational waves (CD-I wave and CD-II wave) propagating through the medium M_1 which we designate as the region $x_3 > 0$ and incident at the plane $x_3 = 0$ with its direction of propagation with angle θ_0 normal to the surface. Corresponding to each incident wave, we get reflected LD-wave, T-wave, CD-I and CD-II waves in medium M_1 and transmitted LD-wave, T-wave, CD-I and CD-II waves in medium M_2 . We write all the variables without bar in medium M_1 and attach bar to denote the variables in medium M_2 as shown in Fig.1.

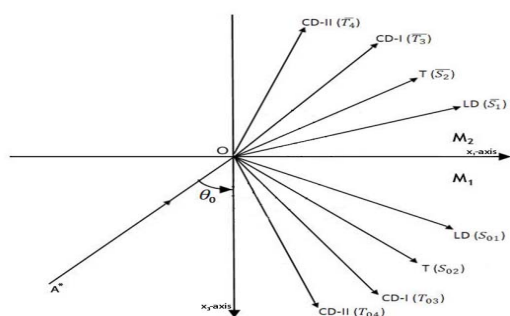


Fig. 1 Geometry of the problem.

In order to solve the Eqs. (13)-(16), we assume the solutions in the form

$$\{\phi, \Phi, \psi, \phi_2\} = \{\tilde{\phi}, \tilde{\Phi}, \tilde{\psi}, \tilde{\phi}_2\} e^{i\{k(x_1 \sin \theta - x_3 \cos \theta) - \omega t\}} \tag{18}$$

Such that k is the wave number, ω is the angular frequency and $\tilde{\phi}, \tilde{\Phi}, \tilde{\psi}, \tilde{\phi}_2$ are arbitrary constants. Using Eq. (18) in Eqs. (13)-(16), we obtain

$$V^4 + D_1 V^2 + E_1 = 0, \tag{19}$$

$$V^4 + D_2 V^2 + E_2 = 0, \tag{20}$$

where

$$D_1 = \frac{-a_3 a_8 (1 - a \omega^2) + i \omega a_3 (\frac{l}{\omega} + a_7) - a_2 a_9}{a_3 a_8}, \quad E_1 = -\frac{a_3 i \omega (\frac{l}{\omega} + a_7) + a \omega^2 (a_3 a_8 + a_2 a_9)}{a_3 a_8}$$

$$D_2 = -\left(\frac{a_1 a_4}{\omega^2} + a_3\right) \frac{1}{a_3 (a_6 - \frac{2a_5}{\omega^2})} - \frac{1}{a_3}, \quad E_2 = \frac{1}{(a_6 - \frac{2a_5}{\omega^2}) a_3}$$

and $V^2 = \frac{\omega^2}{k^2}$

Eqs. (19) and (20) are quadratic in V^2 , therefore the roots of these equations give four values of V^2 . Corresponding to each value of V^2 in Eq. (19), there exist two types of waves in medium M_1 in decreasing order of their velocities, namely LD-wave and T-wave. Similarly corresponding to each value of V^2 in Eq. (20), there exist two types of waves in medium M_1 , namely CD-I wave and CD-II wave. Let V_1, V_2 be the velocities of reflected LD-wave, T-wave and V_3, V_4 be the velocities of reflected CD-I wave, CD-II wave in medium M_1 .

In view of Eq. (14), the appropriate solutions of Eqs. (13)-(16) for medium M_1 and medium M_2 are assumed in the form

Medium M_1 :

$$\{\phi, \Phi\} = \sum_{i=1}^2 \{1, f_i\} [S_{0i} e^{i\{k_i(x_1 \sin \theta_{0i} - x_3 \cos \theta_{0i}) - \omega_i t\}} + P_i], \quad (21)$$

$$\{\psi, \phi_2\} = \sum_{j=3}^4 \{1, f_j\} [T_{0j} e^{i\{k_j(x_1 \sin \theta_{0j} - x_3 \cos \theta_{0j}) - \omega_j t\}} + P_j], \quad (22)$$

where

$$f_i = \frac{-i\omega_i \left[\frac{a_2 a_9}{V_i^2} + a_3 a_8 \left(\frac{1}{V_i^2} - 1 \right) \right]}{\frac{a_2}{V_i^2} \left(\frac{i}{\omega_i} + a_7 \right)}, \quad f_j = \frac{a_3 a_4}{\frac{1}{V_j^2} + ((2a_5 - a_1 a_4) / \omega_j^2) - a_6}$$

and $P_i = S_i e^{i\{k_i(x_1 \sin \theta_i + x_3 \cos \theta_i) - \omega_i t\}}$, $P_j = T_j e^{i\{k_j(x_1 \sin \theta_j + x_3 \cos \theta_j) - \omega_j t\}}$

Medium M_2 :

$$\{\bar{\phi}, \bar{\Phi}\} = \sum_{i=1}^2 \{1, \bar{f}_i\} [\bar{S}_i e^{i\{\bar{k}_i(x_1 \sin \bar{\theta}_i - x_3 \cos \bar{\theta}_i) - \bar{\omega}_i t\}}], \quad (23)$$

$$\{\bar{\psi}, \bar{\phi}_2\} = \sum_{j=3}^4 \{1, \bar{f}_j\} [\bar{T}_j e^{i\{\bar{k}_j(x_1 \sin \bar{\theta}_j - x_3 \cos \bar{\theta}_j) - \bar{\omega}_j t\}}], \quad (24)$$

And S_{0j}, T_{0j} are the amplitudes of incident (LD-wave, T-wave) and (CD-I, CD-II) waves respectively. S_i and T_j are the amplitudes of reflected (LD-wave, T-wave) and (CD-I, CD-II) waves and \bar{S}_i, \bar{T}_j are the amplitudes of transmitted (LD-wave, T-wave) and (CD-I, CD-II) waves respectively.

We use the following extension of the Snell's law to satisfy the boundary conditions

$$\frac{\sin \theta_0}{V_0} = \frac{\sin \theta_1}{V_1} = \frac{\sin \theta_2}{V_2} = \frac{\sin \theta_3}{V_3} = \frac{\sin \theta_4}{V_4} = \frac{\sin \bar{\theta}_1}{\bar{V}_1} = \frac{\sin \bar{\theta}_2}{\bar{V}_2} = \frac{\sin \bar{\theta}_3}{\bar{V}_3} = \frac{\sin \bar{\theta}_4}{\bar{V}_4} \quad (25)$$

where

$$V_j = \frac{\omega}{k_j}, \bar{V}_j = \frac{\omega}{\bar{k}_j} (j=1, 2, 3, 4) \text{ at } x_3 = 0 \quad (26)$$

Making use of the values of ϕ, ψ, Φ and ϕ_2 from Eqs. (21)-(24) in boundary conditions (17) and with the aid of Eqs. (4)-(6), (11), (12), we obtain a system of eight non-homogeneous equations in the following form

$$\sum_{j=1}^8 a_{ij} Z_j = Y_i; \quad (i=1, 2, 3, 4, 5, 6, 7, 8) \quad (27)$$

where the values of a_{ij} are given as:

$$\begin{aligned}
 a_{1i} &= (d_1 + d_2 B_i) \frac{\omega^2}{V_i^2} + (1 + a \frac{\omega^2}{V_i^2}) f_i, & a_{1j} &= d_2 \frac{\omega^2}{V_j V_0} \sin \theta_0 \sqrt{B_j}, \\
 a_{1k} &= - \left[(\bar{d}_1 + \bar{d}_2 R_i) \frac{\omega^2}{V_i^2} + \bar{p}_0 (1 + \bar{a} \frac{\omega^2}{V_i^2}) \bar{f}_i \right], & a_{1l} &= -\bar{d}_2 \frac{\omega^2}{V_j V_0} \sin \theta_0 \sqrt{R_j}, \\
 a_{2i} &= -(2d_3 + d_4) \frac{\omega^2}{V_i V_0} \sin \theta_0 \sqrt{B_i}, & a_{2j} &= (d_3 + d_4) \frac{\omega^2}{V_j^2} B_j - d_3 \frac{\omega^2}{V_0^2} \sin^2 \theta_0 - d_5 f_j, \\
 a_{2k} &= (2\bar{d}_3 + \bar{d}_4) \frac{\omega^2}{V_i V_0} \sin \theta_0 \sqrt{R_i}, & a_{2l} &= - \left[\bar{d}_3 \frac{\omega^2}{V_j^2} \left(1 - 2 \frac{V_j^2}{V_0^2} \sin^2 \theta_0 \right) + \bar{d}_4 \frac{\omega^2}{V_j^2} R_j - \bar{d}_5 \bar{f}_j \right], \\
 a_{3i} &= 0, & a_{3j} &= t \frac{\omega}{V_j} \sqrt{B_j} f_j, & a_{3k} &= 0, & a_{3l} &= t p_1 \frac{\omega}{V_j} \sqrt{R_j} \bar{f}_j, \\
 a_{4i} &= t \frac{\omega}{V_0} \sin \theta_0, & a_{4j} &= -t \frac{\omega}{V_j} \sqrt{B_j}, & a_{4k} &= -t \frac{\omega}{V_0} \sin \theta_0, & a_{4l} &= -t \frac{\omega}{V_j} \sqrt{R_j}, \\
 a_{5i} &= t \frac{\omega}{V_i} \sqrt{B_i}, & a_{5j} &= t \frac{\omega}{V_0} \sin \theta_0, & a_{5k} &= t \frac{\omega}{V_i} \sqrt{R_i}, & a_{5l} &= -t \frac{\omega}{V_0} \sin \theta_0, \\
 a_{6i} &= 0, & a_{6j} &= f_j, & a_{6k} &= 0, & a_{6l} &= -\bar{f}_j, & a_{7i} &= f_i, & a_{7j} &= 0, & a_{7k} &= -\bar{f}_i, & a_{7l} &= 0 \\
 a_{8i} &= t(1 - a_7 t \omega) \frac{\omega}{V_i} f_i \sqrt{B_i}, & a_{8j} &= 0, & a_{8k} &= t p_2 (1 - \bar{a}_7 \omega) \frac{\omega}{V_i} \bar{f}_i \sqrt{R_i}, & a_{8l} &= 0, \\
 d_1 &= \frac{\lambda}{v T_0}, & d_2 &= \frac{(2\mu + K)}{v T_0}, & d_3 &= \frac{\mu}{v T_0}, & d_4 &= \frac{K}{v T_0}, & d_5 &= \frac{K}{\lambda}, \\
 \bar{d}_1 &= \frac{\bar{\lambda}}{v T_0}, & \bar{d}_2 &= \frac{(2\bar{\mu} + \bar{K})}{v T_0}, & \bar{d}_3 &= \frac{\bar{\mu}}{v T_0}, & \bar{d}_4 &= \frac{\bar{K}}{v T_0}, & \bar{d}_5 &= \frac{\bar{K}}{\lambda}, \\
 p_1 &= \frac{\bar{\gamma}}{\gamma}, & p_2 &= \frac{\bar{K}_1}{K_1}, & \bar{p}_0 &= \frac{\bar{v}}{v}, & B_i &= (1 - \frac{V_i^2}{V_0^2} \sin^2 \theta_0), & B_j &= (1 - \frac{V_j^2}{V_0^2} \sin^2 \theta_0), \\
 R_i &= (1 - \frac{V_i^2}{V_0^2} \sin^2 \theta_0), & R_j &= (1 - \frac{V_j^2}{V_0^2} \sin^2 \theta_0)
 \end{aligned} \tag{28}$$

In the above Eq. (28), $i = 1, 2$, $j = 3, 4$, $k = 5, 6$, and $l = 7, 8$

$$Z_1 = \frac{S_1}{A^*}, Z_2 = \frac{S_2}{A^*}, Z_3 = \frac{T_3}{A^*}, Z_4 = \frac{T_4}{A^*}, Z_5 = \frac{\bar{S}_1}{A^*}, Z_6 = \frac{\bar{S}_2}{A^*}, Z_7 = \frac{\bar{T}_3}{A^*}, Z_8 = \frac{\bar{T}_4}{A^*}$$

Such that Z_1, Z_2, Z_3, Z_4 are the amplitude ratios of reflected LD-wave, T-wave and coupled CD-I, CD-II waves in medium M_1 and Z_5, Z_6, Z_7, Z_8 are the amplitude ratios of transmitted LD-wave, T-wave and coupled CD-I, CD-II waves in medium M_2 .

(1) For incident LD-wave:

$$\begin{aligned}
 A^* &= S_{01}, S_{02} = T_{03} = T_{04} = 0, Y_1 = -a_{11}, Y_2 = a_{21}, Y_3 = a_{31} = 0, Y_4 = -a_{41}, Y_5 = a_{51}, \\
 Y_6 &= a_{61} = 0, Y_7 = -a_{71}, Y_8 = a_{81}
 \end{aligned}$$

(2) For incident T-wave:

$$A^* = S_{02}, S_{01} = T_{03} = T_{04} = 0, Y_1 = -a_{12}, Y_2 = a_{22}, Y_3 = a_{32} = 0, Y_4 = -a_{42}, Y_5 = a_{52}, \\ Y_6 = a_{62} = 0, Y_7 = -a_{72}, Y_8 = a_{82}$$

(3) For incident CD-I wave:

$$A^* = T_{03}, S_{01} = S_{02} = T_{04} = 0, Y_1 = a_{13}, Y_2 = -a_{23}, Y_3 = a_{33}, Y_4 = a_{43}, Y_5 = -a_{53}, \\ Y_6 = -a_{63}, Y_7 = a_{73} = 0, Y_8 = a_{83} = 0$$

(4) For incident CD-II wave:

$$A^* = T_{04}, S_{01} = S_{02} = T_{03} = 0, Y_1 = a_{14}, Y_2 = -a_{24}, Y_3 = a_{34}, Y_4 = a_{44}, Y_5 = -a_{54}, \\ Y_6 = -a_{64}, Y_7 = a_{74} = 0, Y_8 = a_{84} = 0$$

6 PARTICULAR CASES

Case I: Energy dissipation without two temperatures

By neglecting two temperature parameters i.e. $a = 0$, $\bar{a} = 0$, we obtain the amplitude ratios at the boundary of two micropolar thermoelastic solid half spaces with energy dissipation. The values of a_{ij} are given by Eq. (28) with the following changed values

$$a_{1i} = (d_1 + d_2 B_i) \frac{\omega^2}{V_i^2} + f_i, \quad a_{1k} = - \left[(\bar{d}_1 + \bar{d}_2 R_i) \frac{\omega^2}{V_i^2} + \bar{p}_0 f_i \right], \quad (i = 1, 2, j = 3, 4, k = 5, 6)$$

Case II: Without energy dissipation

If we take $K_1^* = 0$, $\bar{K}_1^* = 0$, then we obtain the amplitude ratios at the boundary of two micropolar thermoelastic solid half spaces with two temperatures and without energy dissipation and the values of a_{ij} are given in Eq. (28) with the changed values of a_{ij} as:

$$a_{8i} = \iota \frac{\omega}{V_i} f_i \sqrt{B_i}, \quad a_{8k} = \iota p_2 \frac{\omega}{V_i} \sqrt{R_i} f_i, \quad (i = 1, 2, k = 5, 6)$$

Case III: Without energy dissipation and without two temperatures

If we take $K_1^* = 0$, $\bar{K}_1^* = 0$, $a = 0$ and $\bar{a} = 0$, then we obtain the amplitude ratios at the boundary of two micropolar thermoelastic solid half spaces without energy dissipation. The values of a_{ij} are given in Eq. (28) with the changed values of a_{ij} as:

$$a_{1i} = [(d_1 + d_2 B_i) \frac{\omega^2}{V_i^2} + f_i], \quad a_{1k} = - \left[(\bar{d}_1 + \bar{d}_2 R_i) \frac{\omega^2}{V_i^2} + \bar{p}_0 f_i \right], \\ a_{8i} = \iota \frac{\omega}{V_i} f_i \sqrt{B_i}, \quad a_{8k} = \iota p_2 \frac{\omega}{V_i} \sqrt{R_i} f_i, \quad (i = 1, 2, j = 3, 4, k = 5, 6)$$

Case IV: Half-space

If we remove the upper medium M_2 , then we obtain the amplitude ratios at the free surface of micropolar thermoelastic solid half space with two temperatures and energy dissipation as:

$$\sum_{j=1}^4 a_{ij} Z_j = Y_i ; (i = 1, 2, 3, 4)$$

where the values of a_{ij} are given as:

$$\begin{aligned} a_{1i} &= (d_1 + d_2 B_i) \frac{\omega^2}{V_i^2} + (1 + a \frac{\omega^2}{V_i^2}) f_i, & a_{1j} &= d_2 \frac{\omega^2}{V_j V_0} \sin \theta_0 \sqrt{B_j}, \\ a_{2i} &= -(2d_3 + d_4) \frac{\omega^2}{V_1 V_0} \sin \theta_0 \sqrt{B_i}, & a_{2j} &= (d_3 + d_4) \frac{\omega^2}{V_j^2} B_j - d_3 \frac{\omega^2}{V_0^2} \sin^2 \theta_0 - d_5 f_j, \\ a_{3i} &= 0, & a_{3j} &= i \frac{\omega}{V_j} \sqrt{B_j} f_j, & a_{4i} &= i \frac{\omega}{V_i} f_i \sqrt{B_i}, & a_{4j} &= 0 \quad (i = 1, 2, j = 3, 4) \end{aligned}$$

7 NUMERICAL RESULTS AND DISCUSSION

The following values of relevant parameters for both the half spaces for numerical computations are taken.

The values of micropolar constants for medium M_1 are taken from Eringen [39]:

$$\begin{aligned} \lambda &= 9.4 \times 10^{10} \text{ Nm}^{-2}, & \mu &= 4.0 \times 10^{10} \text{ Nm}^{-2}, & K &= 1.0 \times 10^{10} \text{ Nm}^{-2}, \\ \gamma &= 7.79 \times 10^{-10} \text{ N}, & \hat{j} &= 0.002 \times 10^{-17} \text{ m}^2, & \rho &= 1.74 \times 10^3 \text{ Kgm}^{-3}, \end{aligned}$$

and thermal parameters are taken from Dhaliwal and Singh [40]:

$$\begin{aligned} \nu &= 2.68 \times 10^4 \text{ Nm}^{-2} \text{ K}^{-1}, & c^* &= 1.04 \times 10^3 \text{ NmKg}^{-1} \text{ K}^{-1}, \\ a &= 0.5 \text{ m}^2, & T_0 &= 0.298 \text{ K}, & K_1^* &= 1.7 \times 10^2 \text{ Nsec}^{-1} \text{ K}^{-1}, & \omega &= 1. \end{aligned}$$

Following Gauthier [41], the values of micropolar constants for medium M_2 are taken as:

$$\begin{aligned} \bar{\lambda} &= 7.59 \times 10^{10} \text{ Nm}^{-2}, & \bar{\mu} &= 0.0189 \times 10^{12} \text{ Nm}^{-2}, & \bar{j} &= 0.00196 \times 10^{-17} \text{ m}^2, \\ \bar{K} &= 0.0149 \times 10^9 \text{ Nm}^{-2}, & \bar{\gamma} &= 2.68 \times 10^{-5} \text{ N}, & \bar{\rho} &= 2.19 \times 10^3 \text{ Kgm}^{-3}. \end{aligned}$$

Thermal parameters for the medium M_2 are taken as:

$$\begin{aligned} \bar{T}_0 &= 0.0296 \text{ K}, & \bar{K}_1^* &= 1.2 \times 10^2 \text{ Nsec}^{-1} \text{ K}^{-1}, & \bar{\nu} &= 0.02603 \times 10^8 \text{ Nm}^{-2} \text{ K}^{-1}, \\ \bar{c}^* &= 9.21 \times 10^2 \text{ JKg}^{-1} \text{ K}^{-1}, & \bar{a} &= 0.1 \text{ m}^2. \end{aligned}$$

The values of amplitude ratios have been computed at different angles of incidence.

In Figs. 2-25, we represent the solid line for incident wave for thermoelastic solid with two temperatures and with energy dissipation (TS), small dashes line for thermoelastic solid with two temperatures and without energy

dissipation (KTS), large dashes line for thermoelastic solid with energy dissipation (ATS) and dash dot dash line for thermoelastic solid without energy dissipation (AKTS).

7.1 Incident LD-Wave

Variations of amplitude ratios $|Z_i|; 1 \leq i \leq 8$ with the angle of incidence θ_0 , for incident LD-wave are shown in Figs. 2 through 9. Fig. 2 shows that the values of $|Z_1|$ for TS, KTS, ATS and AKTS are oscillatory in the whole range. The values for KTS attain maximum value near the grazing incidence. It is noticed that the values for KTS remain greater than the values for TS in the intermediate range. It is evident from Fig. 3 that the values of amplitude ratio $|Z_2|$ for TS, KTS, ATS and AKTS increase in the whole range, except near the grazing incidence where the values get decreased sharply. Also, the values for KTS in comparison with TS and ATS in comparison with AKTS remain more in the whole range that reveals the effect of energy dissipation. The values of amplitude ratio for TS, KTS, ATS and AKTS are magnified by multiplying by 10. Fig. 4 shows that the values for $|Z_3|$ for TS, KTS, ATS and AKTS increase up to intermediate range and then decrease with further increase in angle of incidence. The values for KTS remain less than the values for TS, ATS and AKTS in the whole range.

Fig.5 depicts that the values of amplitude ratio $|Z_4|$ for TS, KTS, ATS and AKTS increase in the range $0^\circ < \theta_0 < 32^\circ$ and then decrease in the subsequent range. The values of amplitude ratio for TS, KTS, ATS and AKTS are magnified by multiplying by 10^2 . Fig. 6 shows that the behavior of variation of $|Z_5|$ for ATS in comparison with AKTS and TS in comparison with KTS is similar with to difference in their magnitude. The values for TS remain more than the values for ATS in the whole range. The maximum value is attained by KTS near the normal incidence. Fig. 7 shows that the values of $|Z_6|$ for AKTS remain more than the values for ATS in the whole range. The values for KTS and AKTS show sharp decrease near the grazing incidence. The values of amplitude ratio for TS and KTS are magnified by multiplying by 10^5 and 10^6 respectively and the values for ATS and AKTS are magnified by multiplying by 10^4 . It is noticed from Fig. 8 that the values of $|Z_7|$ for TS, KTS and AKTS increase in the range $0^\circ < \theta_0 < 52^\circ$ and then get decreased in the further range. The values of amplitude ratio for ATS and KATS are magnified by multiplying by 10 and the values for KTS are magnified by multiplying by 10^2 . It is noticed from Fig. 9 that values of $|Z_8|$ for KTS remain less than the amplitude for TS in the whole range. The values of amplitude ratio for TS, ATS and AKTS are magnified by multiplying by 10^2 and the values for KTS are magnified by multiplying by 10.

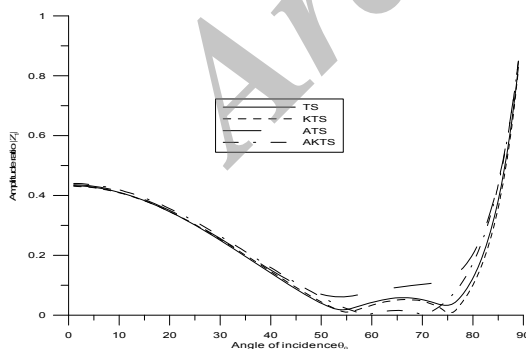


Fig. 2
Variations of amplitude ratios with the angle of incidence for LD-Wave.

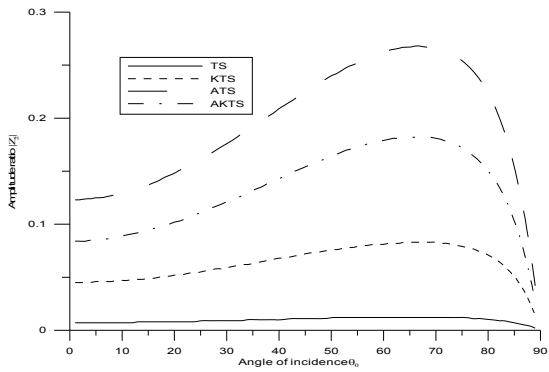


Fig. 3
Variations of amplitude ratios with the angle of incidence for LD-Wave.

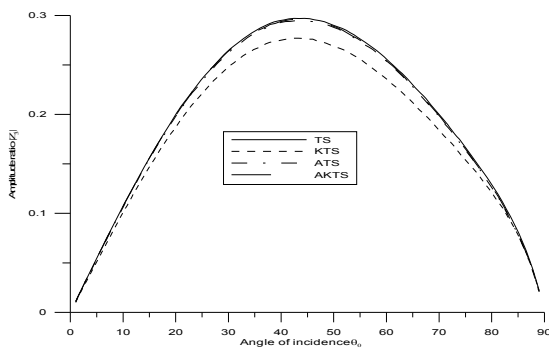


Fig. 4
Variations of amplitude ratios with the angle of incidence for LD-Wave.

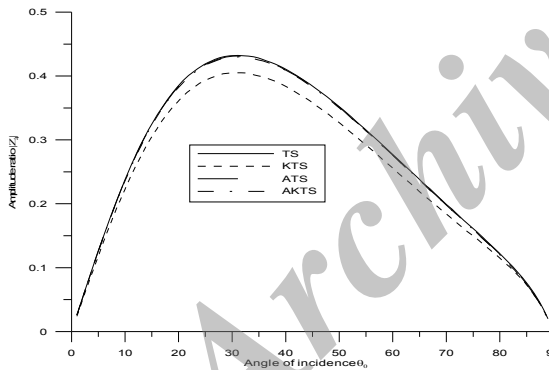


Fig. 5
Variations of amplitude ratios with the angle of incidence for LD-Wave.

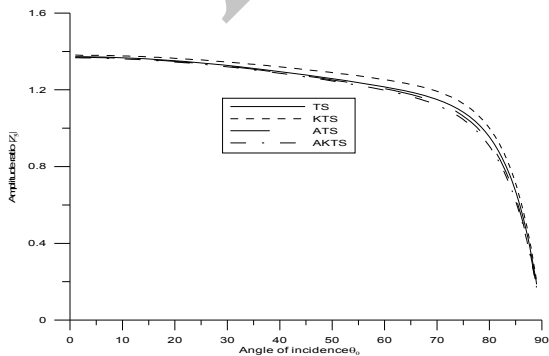


Fig. 6
Variations of amplitude ratios with the angle of incidence for LD-Wave.

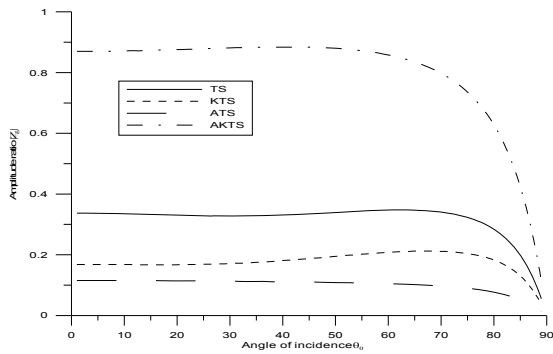


Fig. 7
Variations of amplitude ratios with the angle of incidence for LD-Wave.

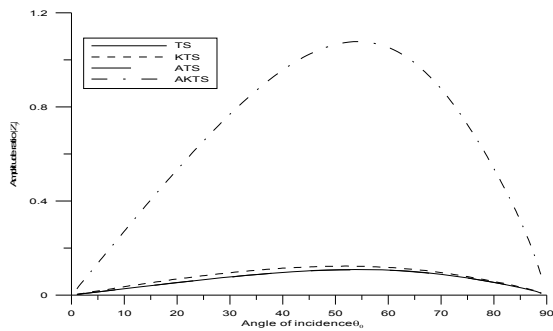


Fig. 8
Variations of amplitude ratios with the angle of incidence for LD-Wave.

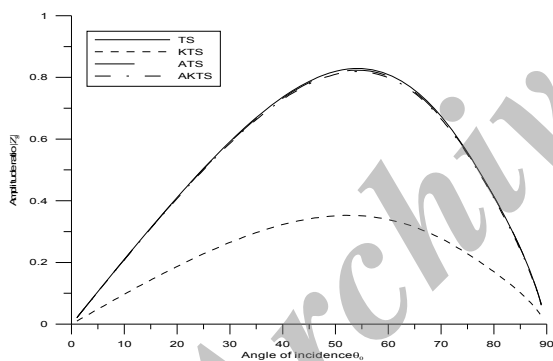


Fig. 9
Variations of amplitude ratios with the angle of incidence for LD-Wave.

7.2 Incident T-Wave

Variations of amplitude ratios $|Z_i|; 1 \leq i \leq 8$ with the angle of incidence θ_0 , for incident T-wave are shown in Figs. 10 through 17. Fig. 10 shows that the values of $|Z_1|$ for TS, KTS, ATS and AKTS oscillate in the whole range. The values for AKTS attain peak value in the interval $20^\circ < \theta_0 < 30^\circ$. The values for KTS are reduced by dividing by 10. Fig. 11 depicts that the amplitude of $|Z_2|$ for TS and KTS increase in the whole range. Also the values for TS in comparison with ATS remain more in the whole range that shows the effect of two temperatures.

It is evident from Fig. 12 that the values of $|Z_3|$ for AKTS attain maximum value in the interval $80^\circ < \theta_0 < 90^\circ$. The values for TS and ATS increase in the range $0^\circ < \theta_0 < 50^\circ$ and then decrease in the remaining range.

Fig. 13 depicts that values of $|Z_4|$ for KTS in comparison with TS are greater. The values of amplitude ratio for TS, KTS, ATS and AKTS are more oscillatory. The values of amplitude ratio for TS, ATS, KTS and AKTS are

magnified by multiplying by 10. Fig. 14 shows that the values of $|Z_5|$ for ATS remain greater than the values for TS in the whole range. The values for AKTS attain peak value in the interval $25^\circ < \theta_0 < 30^\circ$ and near the grazing incidence. The values for AKTS are reduced by dividing by 10. Fig. 15 shows that the values of $|Z_6|$ for TS, ATS and KTS and AKTS decrease with increase in θ_0 and the values for AKTS attain peak value in the interval $25^\circ < \theta_0 < 35^\circ$ and near the grazing incidence. The values of amplitude ratio for TS, ATS and AKTS are magnified by multiplying by 10^3 . Fig. 16 shows that the values of $|Z_7|$ for ATS remain higher than the values of amplitude ratio TS in the whole range that shows the effect of two temperatures. The values of amplitude ratio for TS and ATS are magnified by multiplying by 10 and the values for KTS are magnified by multiplying by 10^2 . Fig. 17 shows that the behavior of variation of $|Z_8|$ is similar as that of $|Z_7|$ with difference in their magnitude values. The values of amplitude ratio for TS, ATS, AKTS by 10^2 and the values for KTS are magnified by multiplying by 10.

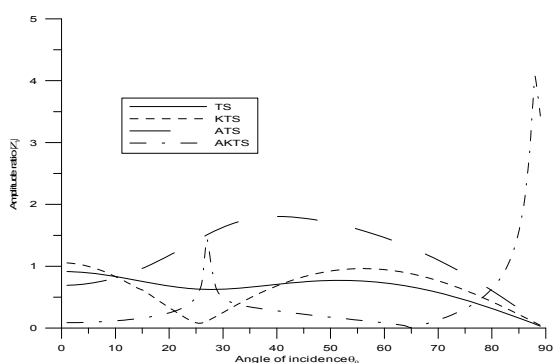


Fig. 10
Variations of amplitude ratios with the angle of incidence for T-Wave.

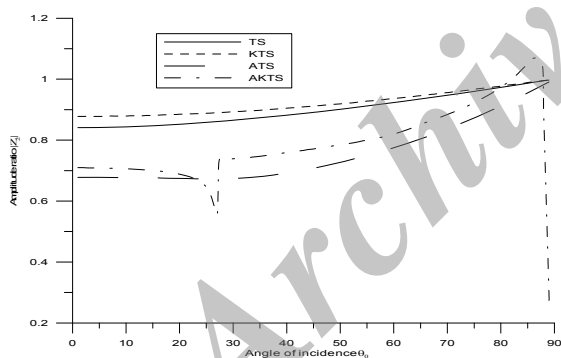


Fig. 11
Variations of amplitude ratios with the angle of incidence for T-Wave.

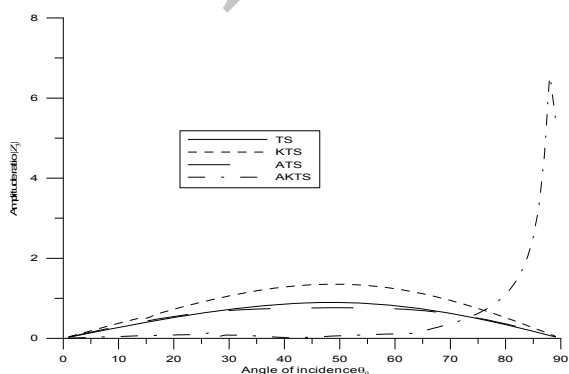


Fig. 12
Variations of amplitude ratios with the angle of incidence for T-Wave.

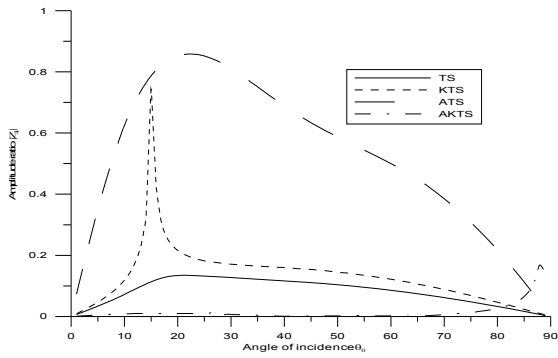


Fig. 13
Variations of amplitude ratios with the angle of incidence for T-Wave.

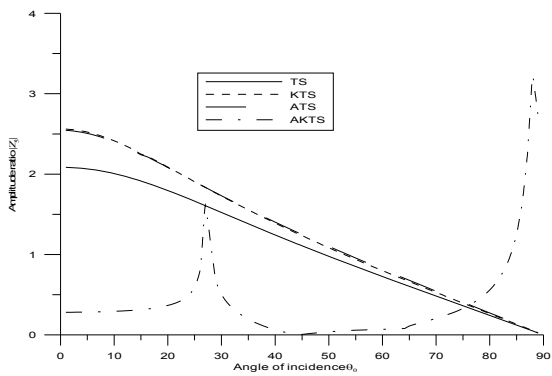


Fig. 14
Variations of amplitude ratios with the angle of incidence for T-Wave.

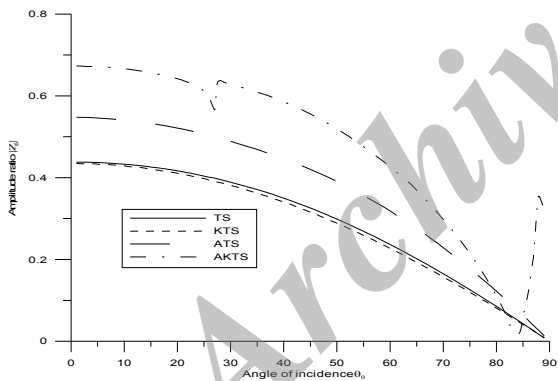


Fig. 15
Variations of amplitude ratios with the angle of incidence for T-Wave.

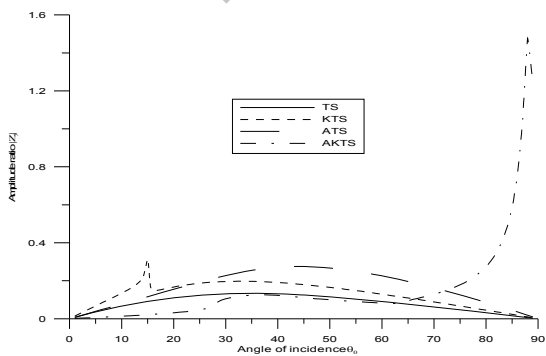


Fig. 16
Variations of amplitude ratios with the angle of incidence for T-Wave.

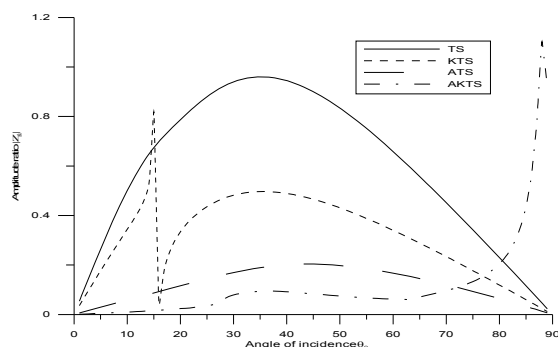


Fig. 17
Variations of amplitude ratios with the angle of incidence for T-Wave.

7.3 Incident CD-I Wave

Variations of amplitude ratios $|Z_i|$; $1 \leq i \leq 8$ with the angle of incidence θ_0 , for incident CD-I wave are shown in Figs. 18 through 25. Fig. 18 depicts that the values of $|Z_1|$ for TS, KTS, ATS and AKTS increase in the interval $0^\circ < \theta_0 < 84^\circ$ and then decrease with increase in θ_0 . The values for TS are greater than the values for KTS, and AKTS in the whole range. It is depicted from Fig. 19 that the values of $|Z_2|$ for AKTS in comparison with KTS are smaller in the whole range. The maximum value is attained by TS in the interval $75^\circ < \theta_0 < 85^\circ$. The values of amplitude ratio for TS, KTS and AKTS are magnified by multiplying by 10^2 and the values for ATS are magnified by multiplying by 10.

It is noticed from Fig. 20 that the values of $|Z_3|$ for TS, ATS and AKTS increase from normal incidence to grazing incidence, except near the grazing incidence, where the values decrease. The values for TS are higher than the values for KTS in the whole range. Fig. 21 depicts that the values of $|Z_4|$ for TS, ATS, KTS and AKTS increase in the whole range. The maximum value is attained by TS at the grazing incidence. There is slight difference in the magnitudes for TS, ATS and AKTS. Fig. 22 shows that the values of $|Z_5|$ for TS in comparison with KTS remain more in the whole range except near the grazing incidence. Fig. 23 depicts that the values of $|Z_6|$ for KTS remain more than the values for TS and the values for ATS remain more than that for AKTS in the whole range due to the dissipation of energy. The values of amplitude ratio for TS and KTS are magnified by multiplying by 10^6 and the values for ATS and AKTS are magnified by multiplying by 10^5 . It is noticed from Fig. 24 that the values of $|Z_7|$ for TS, ATS and AKTS decrease while the values for KTS increase from normal incidence to grazing incidence. There is slight difference in the magnitudes for TS, ATS and AKTS. The values of amplitude ratio for KTS are magnified by multiplying by 10. It is observed from Fig. 25 that behavior of variation of $|Z_8|$ for TS, KTS, ATS and AKTS is similar in the whole range. The values of amplitude ratio for TS, ATS and AKTS are magnified by multiplying by 10^2 .

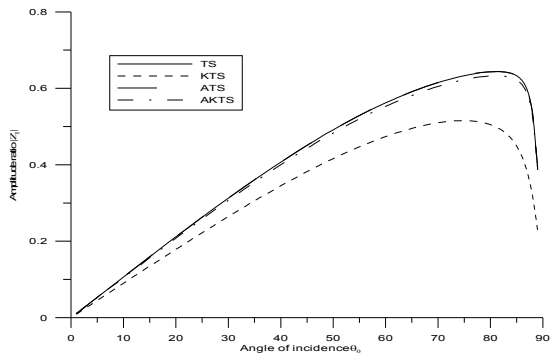


Fig. 18
Variations of amplitude ratios with the angle of incidence for CD-I Wave.

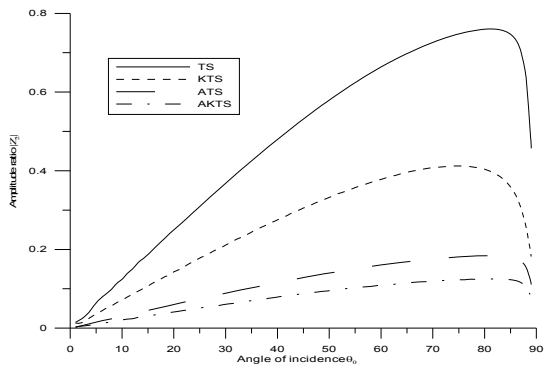


Fig. 19
Variations of amplitude ratios with the angle of incidence for CD-I Wave.

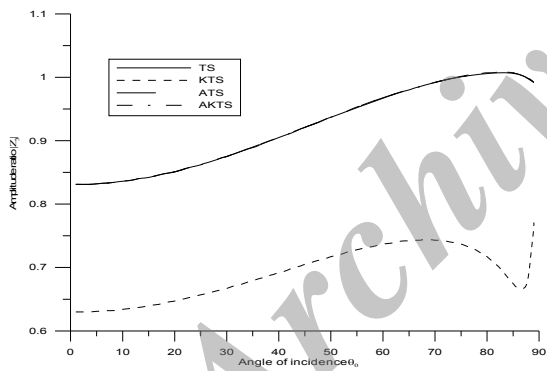


Fig. 20
Variations of amplitude ratios with the angle of incidence for CD-I Wave.

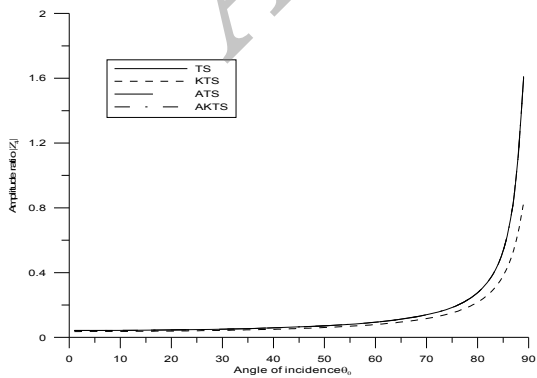


Fig. 21
Variations of amplitude ratios with the angle of incidence for CD-I Wave.

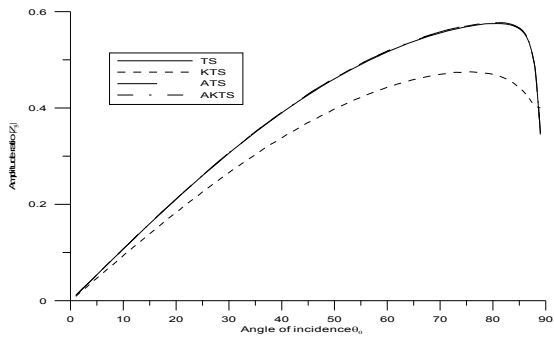


Fig. 22
Variations of amplitude ratios with the angle of incidence for CD-I Wave.

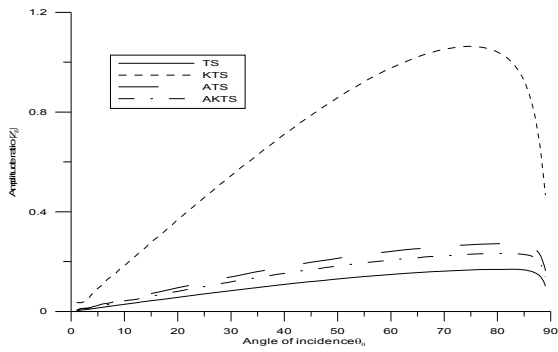


Fig. 23
Variations of amplitude ratios with the angle of incidence for CD-I Wave.

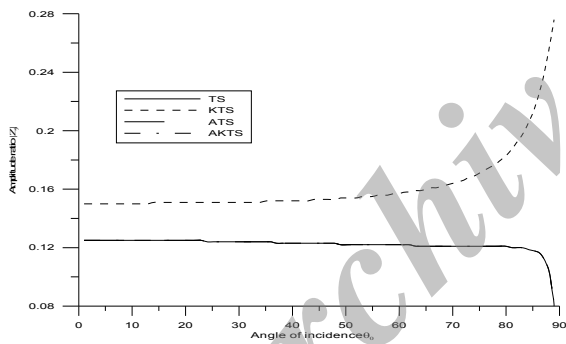


Fig. 24
Variations of amplitude ratios with the angle of incidence for CD-I Wave.

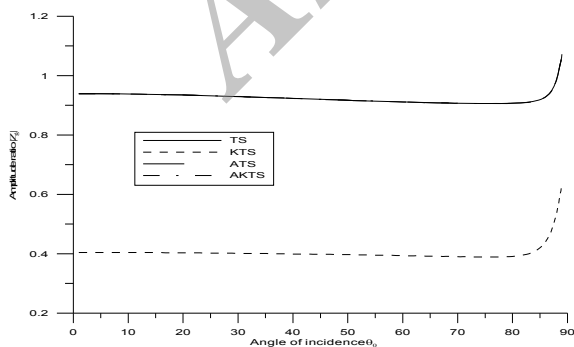


Fig. 25
Variations of amplitude ratios with the angle of incidence for CD-I Wave.

8 CONCLUSIONS

In the present paper, the expressions for reflection and transmission coefficients of various reflected and transmitted waves have been derived in the context of GN type II and GN type III theories. It is observed that when LD-wave is incident, the values of amplitude ratios $|Z_1|, |Z_2|, |Z_5|$ for ATS remain more than the value for TS i.e two temperatures effect decrease the magnitude of amplitude ratios. Also when T-wave is incident, the values of amplitude ratios follow oscillatory pattern and the values for KTS and AKTS attain peak value in the initial range. The values of amplitude ratio $|Z_i|; i = 1, 3, 4$ for TS in comparison with KTS remain greater that reveals the effect of energy dissipation (CD-I wave incident). The problem is of geophysical interest and the results are supposed to be useful in theoretical and observational studies of wave propagation in more realistic models of micropolar solids present in the earth's interior.

REFERENCES

- [1] Eringen A.C., 1966, Linear theory of micropolar elasticity, *Journal of Applied Mathematics and Mechanics* **15**:909-923.
- [2] Eringen A.C., 1970, *Foundations of Micropolar Thermoelasticity*, International Centre for Mechanical Science, Springer-Verlag, Berlin.
- [3] Nowacki W., 1986, *Theory of Asymmetric Elasticity*, Oxford, Pergamon.
- [4] Dost S., Taborrok B., 1978, Generalized micropolar thermoelasticity, *International Journal of Engineering Science* **16**:173-178.
- [5] Chandrasekharaiah D.S., 1986, Heat flux dependent micropolar thermoelasticity, *International Journal of Engineering Science* **24**:1389-1395.
- [6] Boschi E., Iesan D., 1973, A generalized theory of linear micropolar thermoelasticity, *Meccanica* **7**:154-157.
- [7] Boley B. A., Tolins I. S., 1962, Transient coupled thermoelastic boundary value problems in the half-space, *Journal of Applied Mechanics* **29**: 637-646.
- [8] Chen P.J., Gurtin M.E., Williams W.O., 1968, A note on non simple heat conduction, *Zeitschrift für Angewandte Mathematik und Physik* **19**:960-970.
- [9] Chen P.J., Gurtin M.E., Williams W.O., 1969, On the thermoelastic material with two temperatures, *Zeitschrift für Angewandte Mathematik und Physik* **20**:107-112.
- [10] Boley M., 1956, Thermoelastic and irreversible thermodynamics, *Journal of Applied Physics* **27**:240-253.
- [11] Warren W.E., Chen P.J., 1973, Wave propagation in the two temperature theory of thermoelasticity, *Acta Mechanica* **16**:21-23.
- [12] Youssef H.M., 2006, Theory of two temperature generalized thermoelasticity, *Journal of Applied Mathematics* **71**:383-390.
- [13] Kumar R., Mukhopadhyay S., 2010, Effect of thermal relaxation time on plane wave propagation under two temperature thermoelasticity, *International Journal of Engineering Science* **48**:128-139.
- [14] Kaushal S., Sharma N., Kumar R., 2010, Propagation of waves in generalized thermoelastic continua with two temperature, *International Journal of Applied Mechanics and Engineering* **15**:1111-1127.
- [15] Ezzat M.A., Awad E.S., 2010, Constitutive relations, uniqueness of solution and thermal shock application in the linear theory of micropolar generalized thermoelasticity involving two temperatures, *Journal of Thermal Stresses* **33**:226-250.
- [16] Kaushal S., Kumar R., Miglani A., 2011, Wave propagation in temperature rate dependent thermoelasticity with two temperatures, *Mathematical Sciences* **5**:125-146.
- [17] El-Karamany A.S., Ezzat M.A., 2011, On the two-temperature green-naghdi thermoelasticity theories, *Journal of Thermal Stresses* **34**: 1207-1226.
- [18] Banik S., Kanoria M., 2013, Study of two-temperature generalized thermo-piezoelectric problem, *Journal of Thermal Stresses* **36**: 71-93.
- [19] Kumar R., Abbas I. A., 2013, Deformation due to thermal source in micropolar thermoelastic media with thermal and conductive temperatures, *Journal of Computational and Theoretical Nanoscience* **10**: 2241-2247.
- [20] Youssef H. M., 2013, State-space approach to two-temperature generalized thermoelasticity without energy dissipation of medium subjected to moving heat source, *Applied Mathematics and Mechanics* **34**: 63-74.
- [21] Ailawalia P., Lotfy K.H., 2014, Two temperature generalized magneto-thermoelastic interactions in an elastic medium under three theories, *Applied Mathematics and Computation* **227**: 871-888.
- [22] Green A.E., Naghdi P.M., 1991, A re-examination of the basic postulates of thermomechanics, *Proceedings of the Royal Society of London A* **357**:253-270.
- [23] Green A.E., Naghdi P.M., 1992, On undamped heat waves in an elastic solid, *Journal of Thermal Stresses* **15**:253-264.
- [24] Green A.E., Naghdi P.M., 1993, Thermoelasticity without energy dissipation, *Journal of Elasticity* **31**:189-209.

- [25] Taheri H., Fariborz S., Eslami M.R., 2004, Thermoelasticity solution of a layer using the Green-Naghdi model, *Journal of Thermal Stresses* **27**:795-809.
- [26] Mukhopadhyay S., Kumar R., 2008, A problem on thermoelastic interactions in an infinite medium with a cylindrical hole in generalized thermoelasticity III, *Journal of Thermal Stresses* **31**:455-475.
- [27] Mohamed N.A., Khaled A.E., Ahmed E.A., 2009, Electromagneto-thermoelastic problem in a thick plate using Green and Naghdi theory, *International Journal of Engineering and Science* **47**:680-690.
- [28] Chirita S., Ciarletta M., 2010, On the harmonic vibrations in linear thermoelasticity without energy dissipation, *Journal of Thermal Stresses* **33**:858-878.
- [29] Chirita S., Ciarletta M., 2011, Several results in uniqueness and continuous dependence in thermoelasticity of type III, *Journal of Thermal Stresses* **34**:873-889.
- [30] Passarella F., Zampoli V., 2011, Reciprocal and variational principles in micropolar thermoelasticity of type II, *Acta Mechanica* **216**:29-36.
- [31] Abbas I.A., 2013, A GN model for thermoelastic interaction in an unbounded fiber-reinforced anisotropic medium with a circular hole, *Applied Mathematics Letters* **26**: 232-239.
- [32] Ailawalia P., Budhiraja S., Singla A., 2014, Dynamic problem in green-naghdi (Type III) thermoelastic half-space with two temperature, *Mechanics of Advanced Materials and Structures* **21**: 544-552.
- [33] Das P., Kar A., Kanoria M., 2013, Analysis of magneto-thermoelastic response in a transversely isotropic hollow cylinder under thermal shock with three-phase-lag effect, *Journal of Thermal Stresses* **36**: 239-258.
- [34] Kothari S., Mukhopadhyay S., 2013, Some theorems in linear thermoelasticity with dual phase-lags for an anisotropic medium, *Journal of Thermal Stresses* **36**: 985-1000.
- [35] Othman M.I.A., Atwa S.Y., Jahangir A., Khan A., 2013, Generalized magneto-thermo-microstretch elastic solid under gravitational effect with energy dissipation, *Multidiscipline Modeling in Materials and Structures* **9**:145-176.
- [36] Fahmy M.A., 2013, A three-dimensional generalized magneto-thermo-viscoelastic problem of a rotating functionally graded anisotropic solids with and without energy dissipation, *International Journal of Computation and Methodology* **63**: 713-733.
- [37] El-Karamany A.S., Ezzat M.A., 2014, On the dual-phase-lag thermoelasticity theory, *Meccanica* **49**: 79-89.
- [38] Guo F.L., Song J., Wang G.Q., Zhou Y.F., 2014, Analysis of thermoelastic dissipation in circular micro-plate resonators using the generalized thermoelasticity theory of dual-phase-lagging model, *Journal of Sound and Vibration* **333**: 2465-2474.
- [39] Eringen A.C., 1984, Plane waves in non local micropolar elasticity, *International Journal of Engineering Science* **22**:1113-1121.
- [40] Dhaliwal R.S., Singh A., 1980, *Dynamic Coupled Thermoelasticity*, Hindustan Publication Corporation, New Delhi, India.
- [41] Gauthier R.D., 1982, *Experimental Investigations on Micropolar Media*, World Scientific, Singapore.